CrossMark

# High performance humidity sensing properties of indium tin oxide (ITO) thin films by sol–gel spin coating method

B. Murali Babu[1] · S. Vadivel[2]

**Abstract** The tin doped indium oxide (ITO) thin films prepared by sol–gel spin coating method with $In(NO_3)3$ $H_2O$ and $SnCl_4 \cdot 5H_2O$ as indium and tin sources respectively is presented. The as deposited samples were annealed at 500 °C for 2 h in order to improve the crystallinity. The structural, morphological and optical properties of the films were analysed by using X-ray diffraction, scanning electron microscope (SEM), UV–Vis transmission spectra and photoluminescence, spectra analysis. The SEM images ensure the uniform and smooth surface of the as prepared and annealed film. The optical transmittance of more than 85 % has been observed in the UV–Vis region with a band gap of 3.91 and 3.73 eV for the as prepared and annealed films of ITO respectively. The PL spectra reveal that the optical properties were significantly improved due to the annealing effect. The annealed film shows high sensitivity for humidity approximately two order changes in the resistance and the sensitivity increases for different relative humidity from 10 to 90 % due to the physisorption between the water molecules and the surface of the thin films.

✉ S. Vadivel
  vadivel.physics@gmail.com

1   Department of Electrical and Electronics Engineering, Paavai Engineering College, Namakkal, Tamilnadu 637018, India

2   Department of Physics, Paavai Engineering College, Namakkal, Tamilnadu 637018, India

## 1 Introduction

Thin film semiconductors play an essential role in detection, monitoring and control of the pollutants involved in the chemical processes the production of hazardous and harmful vapours [1]. Metal-oxide-based thin film sensors, in spite of their commercial success and decades of research and development, still lack selectivity for different species, and often require high working temperatures. This severely limits their usability and poses long-term reliability problems [2]. The sensitivity of the metal oxide based sensors is dependent on the preparation parameters of the sensitive layer/material [3]. Generally, humidity sensor of these films having nanometer size grain with porous structure, which is most important parameters of their potential application for micro sensors. Moreover this type of nanostructure films are optimal candidates for humidity sensing properties due to the high surface exposed for absorption of water molecules. Indium tin oxide, commonly referred to as tin doped indium oxide (ITO), is degenerate n-type semiconducting material that has wide applications in optics and optoelectronics. These applications include flat panel display devices [4, 5], heat reflecting mirrors [6], and heterojunction solar cells [7]. Indium tin oxide ($In_2O_3$:10 %$SnO_2$) films have been extensively studied in recent years because they exhibit relatively rare combination of high visible transmission and significant electrical conductivity, high substrate adherence, good hardness, and chemical inertness.

ITO thin films deposited on glass substrates by a variety of techniques such as rf sputtering [7, 8] electron beam deposition [9], chemical vapor deposition [10], and spray pyrolysis [11]. Among these, sol–gel dip coating method offers the most possibilities to influence the film properties by modifying the size and structure of the inorganic species

in the sol together with the solvents. Moreover this method is cost effective, yields stable, adherent, uniform and hard films with good reproducibility by a relatively simple process. Most reported literature focused on gas sensing or solar cell application of ITO thin films. Only few reports are available about humidity sensing properties of ITO thin films. The present work consists of ITO thin films and systematically investigation of structural, optical, morphological and humidity sensing properties. To the best of the author's knowledge this is the first preliminary report about humidity sensing properties of ITO thin films by sol–gel spin coating method.

## 2 Experimental procedure

### 2.1 Preparation of ITO thin films

The entire chemicals are of analytical grade which is not further purified. Tin doped indium oxide thin films were fabricated by sol–gel spin coating method with $In(NO_3)\cdot 3H_2O$ and $SnCl_4\cdot 5H_2O$ as indium and tin sources, respectively. In a typical experimental procedure, $In(NO_3)\cdot 3H_2O$ was dissolved in double-distilled water separately to make 0.1 M solution (solution A). Then 0.59 mL (0.50 m mol) of $SnCl_4$ (with initial molar ratio of 8:2 for In:Sn) was dissolved in 10 mL absolute ethanol and it was stirred for 30 min (solution B). The solution B was added drop wise to the solution A and stirring for 30 min. The ammonium solution ($NH_4OH$ as precipitate agent) was added drop wise until the pH value reaches 8. During this process the drop rate must be controlled in order to maintain the chemical homogeneity. Films were grown on 76 mm × 26 mm × 1 mm glass microscope slides which were used as depositing substrates. The glass slides acts as the substrates for depositing ITO films. The slides are cleaned ultrasonically, then with acetone, followed by ethanol and finally, deionized water for 10 min respectively and allowed to air dry. Then, the prepared sol was deposited on the substrate using spin coating technique. Spin parameters, including spin speed and time, were fixed at 2500 rpm and 25 s, respectively. The as deposited samples were annealed at 500 °C for 2 h in order to improve the crystallinity.

### 2.2 Characterization techniques

The prepared samples were successfully characterized by the following techniques. Structural properties of the ITO thin films were analyzed by using X-ray diffraction (XRD, JEOL diffractometer) with monochromatized Cu Kα radiation (λ = 1.54056 Å) in the range of 10°–80° with the step size of 0.1°. The morphology of the ITO thin films is observed by Scanning electron microscope (JEOL Model

JSM-6390LV). The optical transmittance of the thin films was recorded at room temperature by a Perkin Elmer UV/VIS/NIR Lambda 19 spectrophotometer in the wavelength range of 300–900 nm. Photoluminescence spectra of the samples were recorded using PerkinElmer LS 55 Spectrometer equipped with a 40 W Xenon lamp, excitation length used was 325 nm.

## 3 Results and discussion

### 3.1 XRD analysis

Non-destructive X-ray diffraction technique was used to determine the structure and crystalline size of ITO thin films. The XRD pattern both as prepared and annealed films are shown in Fig. 1. Both the samples exhibited to cubic structure of $In_2O_3$ with the space group $La_3$ and the results are in good agreement with the standard JCPDS data (Card No. #06-0416). There is no peak evidence for $SnO_2$ even when it is annealed at 500 °C. This result indicates that Sn atoms are doped into $In_2O_3$ structure. The calculated lattice constants are smaller than the standard $In_2O_3$ (a = 10.081 Å), this is due the $Sn^{4+}$ ionic radius (0.69 nm) is smaller than $In^{3+}$ ionic radius (0.80 nm), which will lead to the decrease of the planar spacing of $In_2O_3$ crystal lattice [12]. The average crystalline sizes of ITO thin films were calculated by using Scherrer's equation [13].

$$d = \frac{K\lambda}{\beta \cos \theta}$$

where d is the mean crystallite size, K is the shape factor taken as 0.89, λ is the wavelength of the incident beam, β is
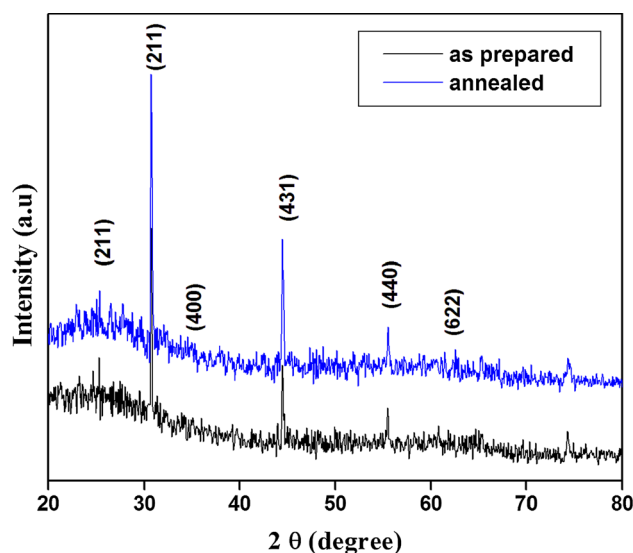


Fig. 1 Shows the XRD Pattern of ITO thin films

the full width at half maximum and θ is the Bragg angle. The average crystalline size was found to be 56 and 67 nm for as prepared and annealed films respectively. The result reveals that calcinations can improve the ITO thin films.

## 3.2 Scanning electron microscope analysis

The morphology and surface of the ITO thin films were analysed by using SEM micrograph. Figure 2 shows SEM images of both pure and as prepared and annealed films respectively. SEM images clearly show the ITO films are nanoclusters with uniform size. There is no change in the morphology but the size of the particles slightly increases by the annealing samples. The increase in grain size of the annealed films is also confirmed by XRD analysis. Number of smaller nanoparticles is composed and forms the clusters on the thin film surface. The average particle size was found to be 55 and 70 nm for as prepared and annealed films of ITO respectively.

## 3.3 UV–Vis spectra analysis

The optical nature and band gap energy of the samples were found out by using UV–Vis transmission spectra analysis. Figure 3a shows the UV–Vis transmission spectra of ITO films. In both the films optical transparency is between 80 and 85 %, but for the annealed films the absorption edge is shifted towards the longer wavelength, which indicates the decrease of the band gap energy. The absorption coefficient (α) was calculated from the transmission spectra using equation [14],

$$\alpha = 1/t \ln(1/T)$$

where T is the optical transmission and t is the thickness of the samples. The indirect band gap of the pure and ITO films was calculated from Fig. 3b using the formula [15],
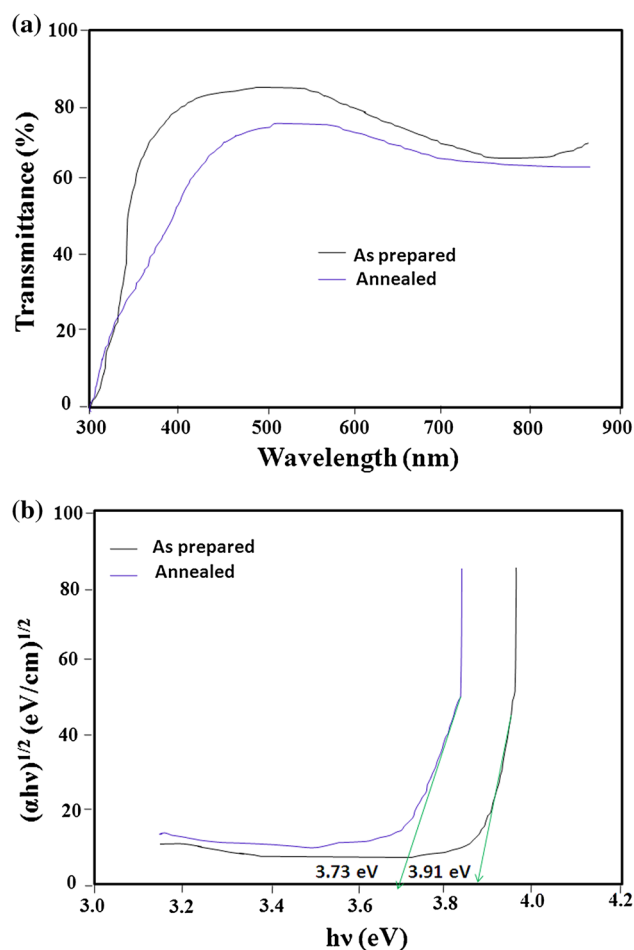
**Fig. 3** UV–Vis spectra of ITO thin films **a** transmittance spectra, **b** band gap energy determination

$$\alpha h\nu = A(h\nu - E_g)^m$$

where α is the absorption coefficient, h is the Planck's constant, ν is the frequency of incident light, $E_g$ is the energy band gap of material and m is the factor governing
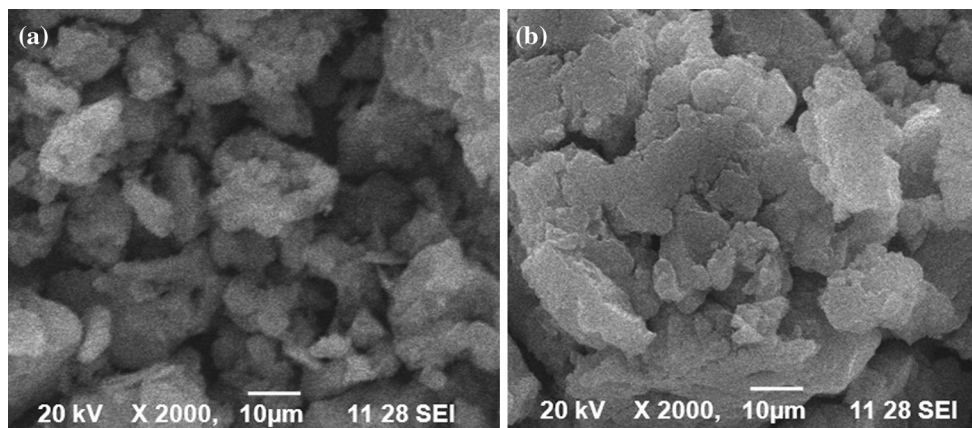
**Fig. 2** SEM micrograph of ITO thin films **a** as prepared, **b** annealed at 500 °C

the direct/indirect, etc. The band gap energy was calculated as 3.91 and 3.73 eV for asprepared and annealed films of ITO respectively.

### 3.4 Photoluminescence spectra analysis

Photoluminescence is a commonly used tool for probing electron–hole surface processes of semiconductor materials, the determination of band-gap energy and surface defect in the samples. Figure 4 shows the PL emission spectra of both as prepared and annealed films of ITO respectively measured from 300 to 600 nm using a 325 nm He–Cd laser. In both pure and doped films, there are series of peaks observed at 359, 411, 446 and 518 nm. The UV emission (359 nm) is also related to near band edge (NBE) emission, and it originates due to the recombination of free exciton through an exciton–exciton collision process [16]. The blue (411 nm) and green emission peaks (518 nm) were attributed to electron transmission, mediated by defect levels in the band gap, such as oxygen vacancies, tin interstitials and so forth.

### 3.5 Humidity sensor set up

The humidity sensor set up was fabricated and their details are explained below. The humidity sensor system consists of quartz glass plates with size 300 mm × 300 mm in dimension and 10 mm thickness provided with top and bottom of the glass plates. There are two holes provided in bottom and top of the glass plates in order to inset and remove the water vapour. In the right upper side of the glass reactor, the vacuum pump is attached to humidify chamber for the next cycle/sample. The electrical
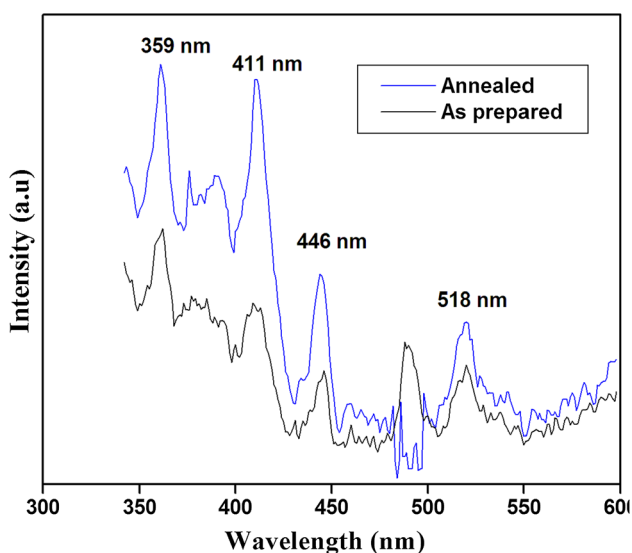
resistance of the sensor material has been measured using LCR Bridge under different humidity conditions. The humidity level varies from 10 to 90 % RH. The percentage of humidity was measured by using standard hygrometer. The ITO thin films and Ohmic contacts were made by silver paste. The schematic diagram of the sensor is given in Fig. 5a and experimental setup is shown in Fig. 5b.

The percentage of sensitivity for detection of humidity is defined as [17]

$$S = \frac{RH_2 - RH_1}{RH_1} \times 100$$

where $RH_2$ is the resistivity of the sample for humidity at level 2 (highest RH level) and $RH_1$ is the resistivity of the sample for humidity at level 1 (lowest RH level).

#### 3.5.1 Humidity sensor test

Figure 6 shows the change in resistance as a function of humidity from 10 to 90 % RH at room temperature. In both as prepared and annealed films the resistance gradually decreases with the increase of relative humidity. The enhanced decrease in resistance or increase in conductance was observed for annealed samples as compared to as prepared films. This could be attributed to improved crystanality and also smaller energy band gap. Figure 7 shows the sensitivity of both as prepared and annealed films as a function of relative humidity. The sensitivity is measured from different relative humidity (RH 10 % to RH 90 %). It is clearly seen that the sensitivity linearly increases with the increase in relative humidity. The
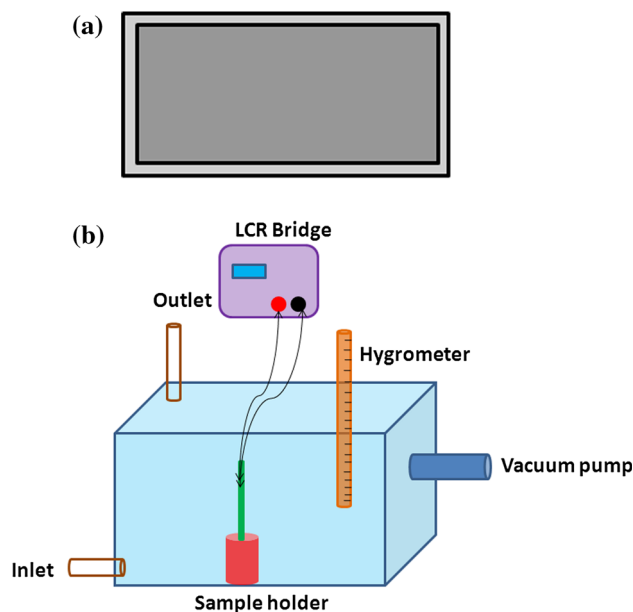


**Fig. 4** Photoluminescence spectra of ITO thin films **a** as prepared, **b** annealed at 500 °C (Color figure online)



**Fig. 5 a** Schematic diagram of the sensor, **b** Humidity sensor experimental setup

**Fig. 6** Change in resistance of ITO thin films as a function of relative humidity
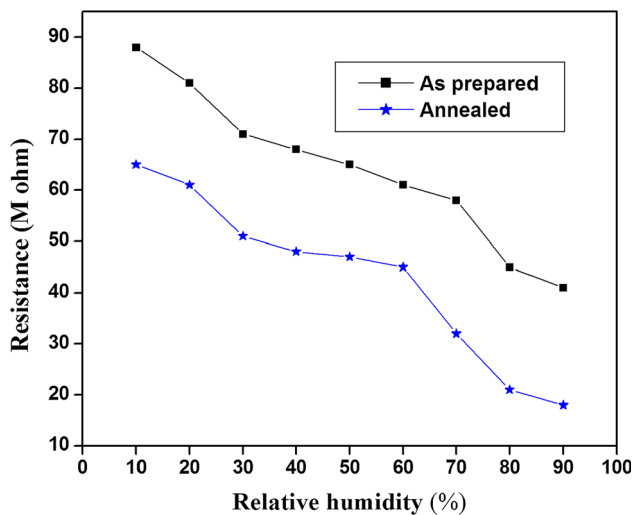


**Fig. 8** Response and recovery time of ITO thin films as a function of relative humidity
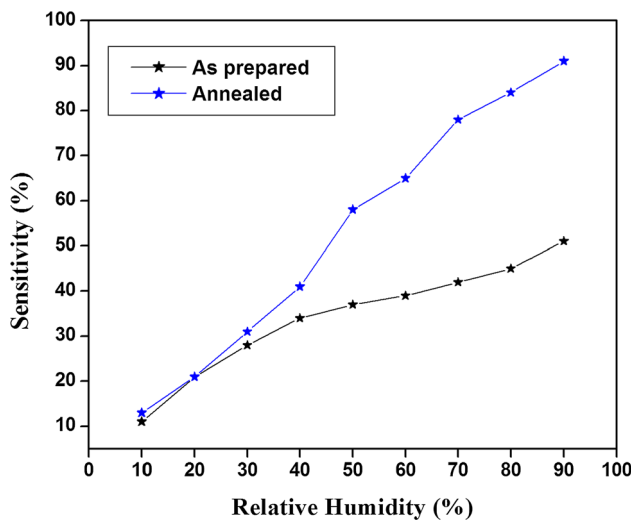


**Fig. 7** Sensitivity of ITO thin films as a function of relative humidity

annealed film shows high sensitivity and more stability as compared to as prepared films. Figure 8 shows the response and recovery curves for both as prepared and annealed films. The response and recovery behavior is one of the most important characteristic for evaluating the humidity sensors [18]. The average response time of as prepared film is 75 s and recovery time is 65 s, similarly the average response and recovery time for 58 and 45 s for annealed films. Hence our studies suggest that ITO films can be a promising material for high performance humidity sensing applications. In both films exhibit a decrease in resistance or increase in conducting property with increasing RH%. This could be attributed to water vapour chemisorbs on the surface of the sensor. The electrical response will depend on the number of water molecules
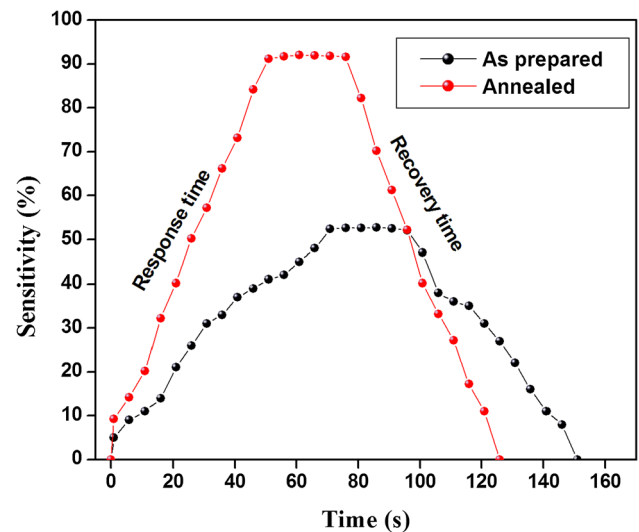
adsorbed on the surface of the sensor films [19]. Water is then physically adsorbed on top of the chemisorbed layer of the ITO film and then further physisorbed layers will be formed. The physically adsorbed water molecules on the surface of the thin sensing film play a dominating role for the humidity sensing mechanism. Moreover, annealed films of ITO show better sensing performance as compared with as prepared films. This could be due to more electrons are depleted in the films and it easily extracts an electron from the conduction band and increases the conductance of the sensor at different RH%. This action is observed in the case of bigger diameter grains (annealed films) because the grain boundaries will be more compared with the smaller diameter grains (as prepared films).

## 4 Conclusion

The preparation of ITO thin films using sol–gel spin coating method has been reported and its structural and optical properties were analysed. The thin film samples exhibit the cubic structure of $In_2O_3$ with the space group $La_3$ and the results are in good agreement with the standard JCPDS data (Card No. #06-0416). The UV and PL results show that the optical properties of the ITO films have been significantly improved for annealed samples. The humidity sensing test performed on annealed films under various humidity levels from 10 to 90 % RH at room temperature demonstrates high sensitivity, faster response and recovery time of 58 and 45 s respectively. The developed ITO thin films can be used as high performance humidity sensor and gas sensor devices under room temperature.

# References

1. L.I.B. Silva, T.A.P. Rocha-Santos, A.C. Duarte, Glob. Nest J. **10**, 217–225 (2008)
2. G.S. Aluri, A. Motayed, A.V. Davydov, V.P. Oleshko, K.A. Bertness, N.A. Sanford, M.V. Rao, Nanotechnology **22**, 295503 (2011)
3. M. Fleischer, H. Meixner, Sens. Actuators B **43**, 1–10 (1997)
4. J.E. Costellamo, *Handbook of Display Technology* (Academic Press, New York, 1992)
5. S. Ishibashi, Y. Higuchi, Y. Ota, K. Nakamura, J. Vac. Sci. Technol. **A8**, 1399 (1990)
6. K.L. Chopra, S.R. Das, *Thin Film Solar Cells* (Plenum Press, New York, 1983), p. 321
7. C.V.R. Vasant Kumar, A. Mansingh, J. Appl. Phys. **65**, 1270 (1989)
8. S.A. Knickerbocker, A.K. Kulkarni, J. Vac. Sci. Technol. **A13**(3), 1048 (1995)
9. S.A. Agnihotry, K.K. Sari, T.K. Saxena, K.C. Nagpal, S. Chandra, J. Phys. D Appl. Phys. **18**, 2087 (1985)
10. K.L. Chopra, S. Major, D.K. Pandya, Thin Solid Films **102**, 1 (1983)
11. J.C. Manifacier, L. Szepessy, J.F. Bresse, M. Perotin, R. Stuck, Mater. Res. Bull. **14**, 163 (1979)
12. A. Walsh, J.L.F. Da Silva, S.H. Wei, Phys. Rev. B **78**(7), 075211 (2008)
13. M. Parthibavarman, K. Vallalperuman, S. Sathishkumar, M. Durairaj, K. Thavamani, J. Mater. Sci. Mater. Electron **25**, 730 (2014)
14. Z.S. Seddigi, Bull. Environ. Contam. Toxicol. **84**, 564 (2010)
15. X.C. Song, E. Yang, G. Liu, Y. Zhang, Z.S. Liu, H.F. Chen, Y. Wang, J. Nanopart. Res. **12**, 2813 (2010)
16. A. Umar, B. Karunagaran, E.K. Suh, Y.B. Hahn, Nanotechnology **17**, 4072 (2006)
17. S.C. Nagaraju, A.S. Roy, J.B. Prasanna Kumar, K.R. Anilkumar, G. Ramagopal, J. Eng. (2014). doi:10.1155/2014/925020
18. M. Parthibavarman, V. Hariharan, C. Sekar, Mater. Sci. Eng. C **31**, 840–844 (2011)
19. G. Gusmano, G. Montesperelli, E. Traversa, A. Bearzottti, Sens. Actuators B **14**, 525–527 (1993)